Available online at www.sciencedirect.com
SCIENCE DIRECT
Polymer 47 (2006) 5314–5322
polymer
www.elsevier.com/locate/polymer

Sub-micrometer polyamide droplets dispersed in polyethylene: Dimensional stability above the melting point of polyethylene

Manuel Salmerón Sánchez [a,*], Vincent Mathot [b,c], Gabriel Groeninckx [b], Willie Bruls [d]

[a] Center for Biomaterials, Universidad Politécnica de Valencia, Camino de Vera s/n, 46022 Valencia, Spain
[b] Division of Molecular and Nanomaterials, Laboratory for Macromolecular Structural Chemistry, Department of Chemistry, Katholieke Universiteit Leuven, Celestijnenlaan 200F, B-3001, Heverlee, Belgium
[c] SciTe, Ridder Vosstraat 6, 6162 AX Geleen, The Netherlands
[d] DSM Research, P.O. Box 18, 6160 MD Geleen, The Netherlands

Received 6 May 2005; received in revised form 5 May 2006; accepted 8 May 2006
Available online 14 June 2006

Abstract

Metallocene-catalyst polymerized ethylene-1-octene copolymers in which a polyamide 6 (PA6) is finely dispersed by means of a MA-grafted-polyethylene as compatibilizer show a non-conventional mechanical behavior at high temperatures. Once the ethylene-1-octene copolymer is melted the system still shows good mechanical properties and dimensional stability. Besides, due to the dispersed phase morphology of the system, so-called fractionated/homogeneous crystallization takes place (extra supercooling of around 50 °C compared to the bulk PA6 crystallization temperature) and the material can be processed in the same temperature range in which it later on will show good mechanical response. The explanation of this intriguing mechanical behavior is sought in the molecular architecture of the system and turns out to be related to the slower flow dynamics of the matrix chains in case of high enough molar mass. The slower dynamics is caused by an increase in entanglement density due to mixing/interactions between matrix chains and compatibilizer chains chemically attached to the droplets. The droplets thereby function as physical crosslinks.

Keywords: Ethylene-1-octene copolymers; Polyamide; Mechanical properties

1. Introduction

Polymer blending is a convenient way for obtaining new materials whose properties are better than just a simple superposition of those of the individual components. Because it is also cheaper and less time-consuming the method is more efficient than synthesis of new monomers or inventing new polymerization strategies. Miscible polymer blends are the exception rather than the rule and most polymeric blends are immiscible due to the positive values of the mixing Gibbs free energy. In many incompatible blends one of the components is dispersed as minor phase into the other that acts as matrix. As the adhesion between the two phases is crucial for the application envisaged, in most cases the system must be somehow compatibilized.

This work investigates the system obtained by dispersing a polyamide 6 (PA6), by means of a polyethylene-grafted-maleic anhydride (PE-*g*-MA) as compatibilizer in an ethylene-1-octene copolymer matrix. The special morphology of the system makes it interesting both from a fundamental and an applied perspective. From the fundamental point of view the system shows two outstanding characteristics, on the one hand the very fine dispersion of the PA6 droplets makes the system appropriate for studying the phenomenon of fractionated/homogeneous crystallization. On the other hand, the system shows a peculiar mechanical behavior at high temperatures: once the matrix has melted the sample still shows good mechanical properties [1]. This paper concerns mainly the last issue. It is precisely this intriguing mechanical phenomenon what makes the system attractive from the application point of view because it allows extending the use of ethylene-1-octene copolymers for applications where dimensional stability is required above their melting point. Moreover, due to the fractionated/homogeneous crystallization phenomenon the material can be processed at lower temperatures, in the same range in which it later on will show good mechanical properties.

* Corresponding author. Tel.: +34 963877275; fax: +34 963877276.
E-mail address: masalsan@fis.upv.es (M. Salmerón Sánchez).

0032-3861/$ - see front matter © 2006 Elsevier Ltd. All rights reserved.
doi:10.1016/j.polymer.2006.05.016

The mechanical behavior of polyethylene/PA6 incompatible blends has been extensively studied in the literature. Kudva et al. investigated blends in a broad range of compositions including the effect of the incorporation of PE-*g*-MA [2]. However, these authors focused on the improvement of the impact strength at moderate temperatures (below 80 °C). Impact strength and mechanical properties at room temperature have also been studied for this type of blend using different compatibilizers [3–12]. Minkova et al. studied blends of LDPE and PA6 with two types of functionalised polyethylene as compatibilizer, but focused on PA6 as the co-continuous phase and on the effect on microhardness at room temperature [13]. Bai et al. studied PP/PA6 blends employing PE-*g*-MA as compatibilizer. For PA6 contents from 0 to 40%, a dispersed phase morphology consisting of PA6 droplets was obtained. However, the mechanical properties were only studied below the melting temperature of the matrix [14]. Okada et al. studied the mechanical properties of blends of maleated ethylene–propylene rubber and PA6 at room temperature [15,16]. Tedesco et al. studied the system PP/PP-*g*-MA/PA6 in the ratio 63/7/30 (very close to the composition of our blends, see the Section 2) but they too did not consider the mechanical properties above the melting temperature of the matrix [17].

Many more references [18–26] describe the blending of PA with hydrocarbon elastomers and the effect of compatibilization through grafting of maleic anhydride on the polyethylene phase. However, the peculiar mechanical behavior of our system has not been previously reported for a blend with dispersed phase morphology.

In this work, we have dispersed the same percentage of PA6 in two ethylene-1-octene copolymers of different viscosities, i.e. different molar masses, using the same percentage of PE-*g*-MA as compatibilizer in each case. The two main goals of this paper are (i) to show and characterize for the first time a system with a dispersed droplet morphology that is able to keep good mechanical properties (modulus high enough as to maintain dimensional stability) above the melting point of the matrix, (ii) to explain the possible molecular origin of this phenomenon.

2. Experimental

2.1. Materials

The main characteristics of the polymers used in this work are listed in Table 1. Ethylene-1-octene copolymers (Exact® Plastomers 8201, 8210) with different melt flow index (MFI) were supplied by DEX-PLASTOMERS. These commercial available copolymers are homogeneous ones: the way the comonomer is incorporated during polymerization can be described by one single set of chain propagation probabilities of comonomer incorporation in the chain (P-set) per copolymer or, alternatively, by the combination of a single set of reactivity ratios (r-set) for all copolymers and a single monomer/comonomer ratio for each copolymer. Statistically there are no differences within and between the molecules (see [27] and references therein).

Table 1
Molecular characteristics of the materials

Material	MFI (dg/min)[a]	M_w (kg/mol)	$D^{23\ °C}$ (kg/m^3)
Exact 8201	1	115	882
Exact 8210	10	72	882
PE-*g*-MA	–	65	–
PA6	–	24	–

Note. MMD for Exact grades calculated using universal calibration. MMD figures for PE-*g*-MA calculated using conventional calibration.
[a] Melt flow index 230 °C/5 kg.

Polyamide 6 (PA Akulon K123) was provided by DSM Engineering Plastics. Polyethylene grafted maleic anhydride (PE-*g*-MA) used as compatibilizer (Fusabond® N MO525D) was supplied by DuPont.

2.2. Blends preparation

Two different blends were prepared, keeping the same matrix/dispersed phase/compatibilizer ratio (62.5/30/7.5), while the characteristics of the matrix were changed. The matrix was in each case an ethylene-1-octene copolymer (Exact® 8201, 8210) with a different melt flow index, MFI, indicated by the two last numbers in the name (Table 1). Polyamide 6 was used as the dispersed phase. The compatibilizer agent was PE-*g*-MA. Blends were prepared on a Haake 60 cc batch mixer under polyamide 6 normal processing conditions. Before processing all materials were dried overnight at 80 °C under vacuum with a nitrogen flow leak. All blends were mixed at 240 °C at a screw speed of 80 rpm. During melt blending the mixing chamber was kept saturated with N_2 gas to avoid oxidative degradation.

The blends studied in this work using as matrix the above mentioned ethylene-1-octene copolymers 8201 and 8210 will be called B1 and B2, respectively.

2.3. Dissolution experiments

The morphology of the blends was analyzed by means of dissolution experiments to determine whether the extruded blends displayed a droplet/matrix or a co-continuous phase morphology. Small pieces of the samples were immersed in toluene (at 50 °C) and formic acid (at room temperature) under stirring conditions for several days. Formic acid is a solvent for PA6 and a non-solvent for the ethylene-1-octene copolymer. Toluene is a solvent for ethylene-1-octene copolymers and a non-solvent for PA6.

2.4. Transmission electron microscopy (TEM) and image analysis

TEM micrographs were made on a Philips CM10, operating at 80 kV. Sections of 100 nm were prepared with a diamond knife (Drukker, International) on a Leica Ultracut UCT microtome, equipped with a Leica EM FCS cryo unit. The temperature of the sample and knife was set to be −80 and −60 °C, respectively. The microtomed sections were collected

in a water/dimethylsulfoxide (40/60 wt%) filled boat attached to the diamond knife. The sections were collected on copper TEM grids and dried on filter paper. The cuts on the grid were stained using a phosphotungstic acid solution 2-wt% for 30 min to increase the contrast between the phases.

Image analysis on the obtained TEM micrographs was performed using Leica Qwin image analysis software. The average sizes and the size distribution of the dispersed droplets were determined. About 1000 droplets were analyzed for each blend in at least five different areas of the samples what allows calculating the number fraction of droplets in a given diameter interval as well as the standard deviation. The number average droplet diameter (D_n), volume average diameter (D_v) and the polydispersity ($P = D_v/D_n$) were calculated from

$$D_n = \frac{\sum n_i d_i}{\sum n_i} \quad (1)$$

$$D_v = \frac{\sum n_i d_i^4}{\sum n_i d_i^3} \quad (2)$$

where n_i is the number of droplets having diameter d_i. These diameters were not corrected to take into account that not all the droplets were cut at their largest cross-section.

2.5. Dynamic mechanical thermal analysis (DMTA)

DMTA was performed using a DMA 2980 apparatus (TA Instruments) at the frequency of 1 Hz in the single cantilever mode. The temperature dependence of the storage modulus (E') and loss angle (tan δ) was measured in the temperature range from -100 to 230 °C at a rate of 2 °C/min. The samples for these experiments were rectangular, approximately $25 \times 10 \times 1$ mm^3 and pre-dried in a vacuum oven at 90 °C.

2.6. Rheology

Experiments were performed in a parallel plate ARES LS rheometer (Rheometric Scientific) at a function of frequency (from 10^{-1} to 10^2 s^{-1}) at different temperatures (120, 150, 180 and 230 °C). The samples for these experiments were discs 24 mm diameter and 1.8 mm thickness, pre-dried in a vacuum oven at 90 °C. A fresh sample was used at each temperature. Besides, a temperature sweep was performed at 0.2 Hz in the range 60–230 °C at a rate of 5 °C/min.

2.7. Differential scanning calorimetry (DSC)

Samples having masses around 5 mg were prepared. Differential scanning calorimetry (DSC) experiments were performed using a Pyris 1 apparatus (Perkin Elmer). Nitrogen gas was led through the cell with a flow rate of 20 ml/min. The temperature of the equipment was calibrated by using indium and zinc. The melting heat of indium was used for energy calibration. The samples were subjected to a heating scan from room temperature up to 250 °C at 10 °C/min and kept at this temperature for 3 min to erase the previous thermal history. Then, the samples were cooled at 10 °C/min to -20 °C and subsequently heated again to 250 °C at the same scanning rate. These last scans are those discussed in the text. Liquid nitrogen was used for cooling at temperatures lower than ambient.

3. Results and discussion

Although TEM images for the different blends (Fig. 1) seem to show that the degree of dispersion of the PA6 droplets hardly depends on the matrix used, i.e. on its physical characteristics, when image analysis of TEM micrographs is done for calculating the droplet size distribution a slight different behavior is obtained. Fig. 2 shows frequency histograms whose main parameters are given in Table 2. The morphologies of B1 and B2 are somehow different in the sense that a unimodal distribution for B1 transforms into a bimodal one for B2 within a matrix of lower viscosity, higher MFI. The width and shape of the droplet size distribution has been related to the viscosity ratio (viscosity of the dispersed phase/viscosity of the matrix) of the melt [28]. A broader droplet distribution is expected as the viscosity ratio increases.

Fig. 3 shows the DSC curves in cooling and heating at 10 °C/min for the different blends. The thermal behavior of the matrix is quite similar in each sample: broad peaks both on cooling and heating, similar to what is obtained for the base

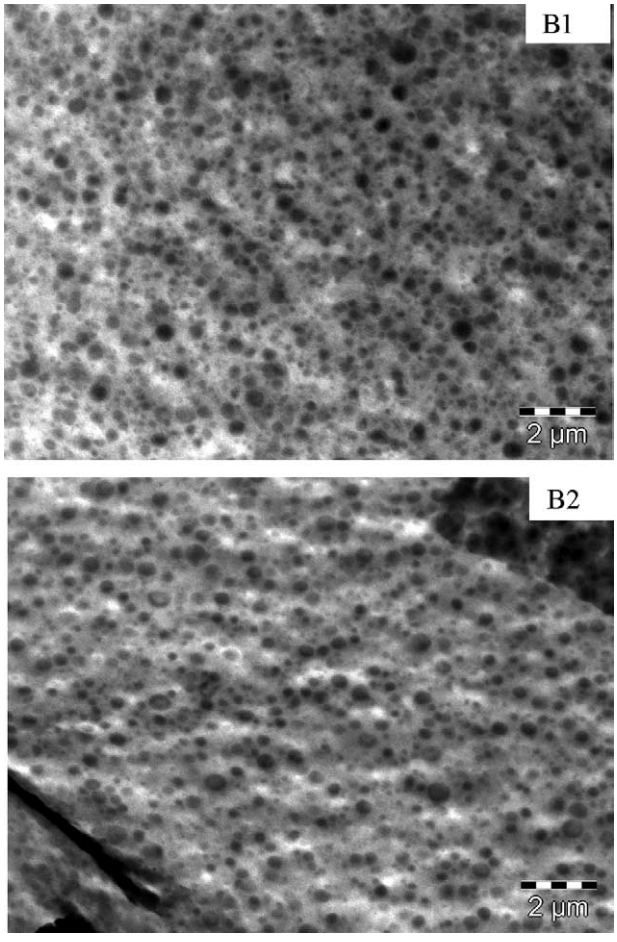

Fig. 1. TEM micrographs of the different blends.

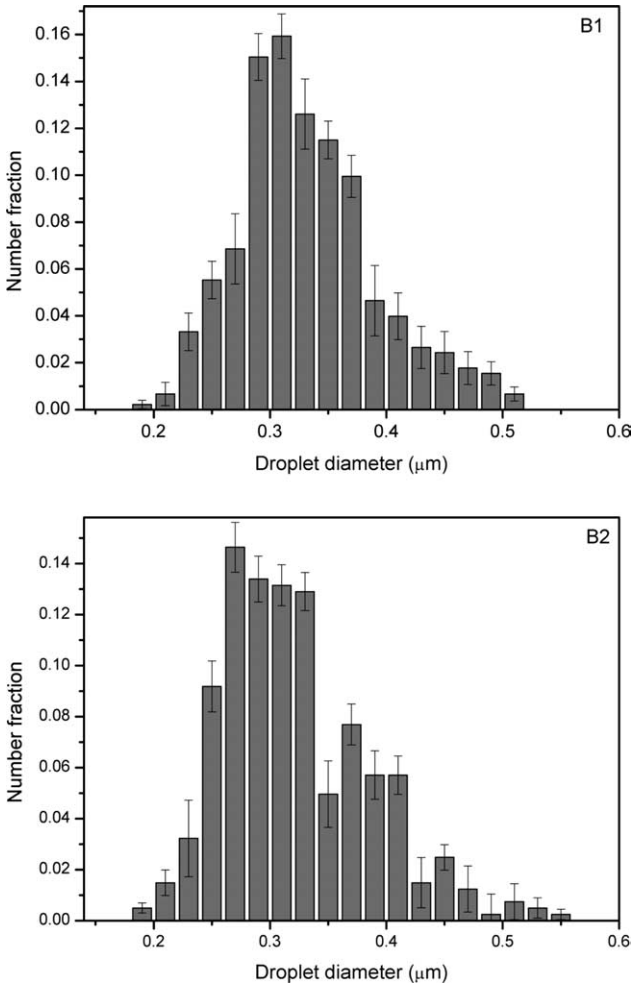

Fig. 2. Droplet size distributions for the different blends.

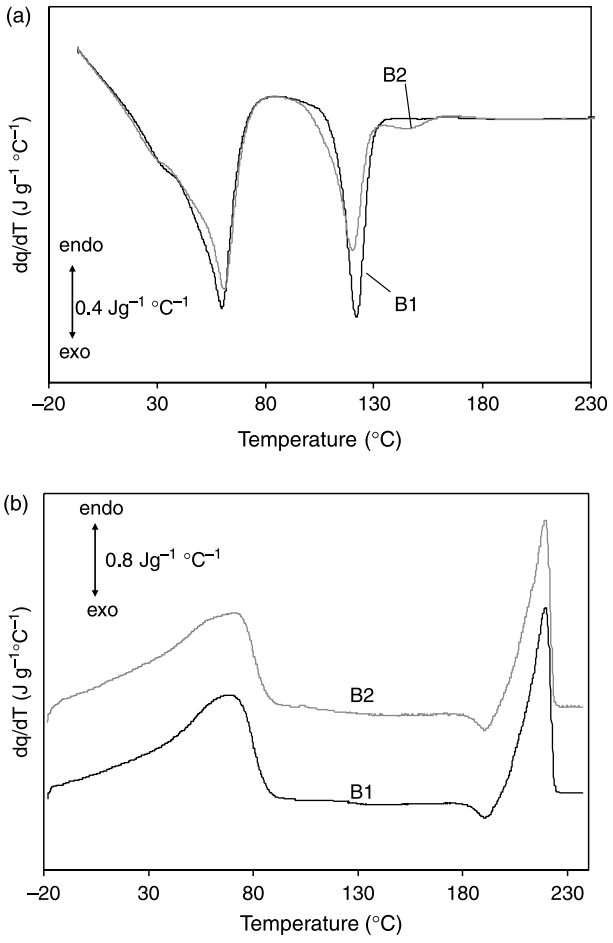

Fig. 3. DSC curves on cooling (a) and heating (b) at 10 °C/min for the different blends. The curves in (b) are shifted for clarity.

ethylene-1-octene copolymers. For such copolymers the broad DSC peaks and their origins have been studied extensively in recent years, see, e.g. [29]. The peaks reflect the crystallization and melting transitions during cooling and heating, which transitions reflect in essence the (dis)appearance of the morphology with respect to the crystallite dimension distribution [30,31]. This distribution originates from the ethylene sequence length distribution [32], which is fixed and known from the P-set per copolymer or from the r-set for all copolymers and the feed per copolymer.

The situation differs as the PA6 dispersed phase concerns, in which crystallization takes place at much lower temperatures (120–130 °C) compared to the PA6 bulk crystallization temperature (170–180 °C), resulting in an extra supercooling of approximately 50–60 °C. The droplet size distribution is reflected in the DSC curves and some differences are found in the crystallization behavior of the two blends: while a well-defined single exotherm is found for B1 at 120 °C, two crystallization peaks appear for B2 (one small at 143 °C, one bigger at 119 °C). Higher supercoolings in dispersed systems are usually explained by the so-called fractionated/homogeneous crystallization phenomenon (for an overview see [33–36]): when the material is dispersed in droplets, heterogeneous nucleation will take place in each one of the droplets and these will crystallize according to the number and type of heterogeneities in it. If the number of droplets is high enough, nucleation in part of the droplets can be dominated by heterogeneities having a higher specific interfacial energy than the nuclei active in bulk conditions, what will decrease their crystallization temperature. Extending this way of reasoning to the extreme leads to a crystallization process via homogeneous nucleation: droplets containing no heterogeneities at all are able to undergo homogeneous nucleation at the largest degree of supercooling. Based on this sketch it has been suggested that the shape of the DSC exotherms in dispersed systems is related to the shape of the droplet size distribution [28,37]. Although the physics behind this relationship deserves further investigation, some correlations are found also in our blends. B1 shows a single exotherm and a unimodal droplet

Table 2
Morphological parameters of the blends

Blend	D_n (μm)	SD_{Dn} (μm)	D_v (μm)	P
B1	0.32	0.06	0.37	1.16
B2	0.33	0.06	0.37	1.12

Number average droplet diameter (D_n) and its standard deviation (SD_{Dn}), volume average droplet diameter (D_v) and polydispersity ($P = D_v/D_n$).

size distribution with a well-defined maximum. The situation is somehow different for B2 in which having droplets in the same size interval as B1, the distribution seems to be the superposition of two peaks (one smaller around 0.4 μm and the other bigger around 0.3 μm). Nevertheless, melting of the PA6 droplets in the two blends is quite similar and it takes place at temperatures close to that of the bulk polyamide.

Fig. 4 shows the storage modulus (E') and mechanical loss tangent (tan δ) for two of the base components: ethylene-1-octene copolymer and PA6. Broad mechanical relaxations are found for the ethylene-1-octene copolymer, around 100 °C in width, and for the PA6 between 60 and 100 °C. However, of interest for this work, it is seen that the modulus of ethylene-1-octene copolymer drops above 100 °C, once the irreversible flow of the polymer chains starts in the melt state, which is expected for a system that is not chemically crosslinked. A similar behavior is found for the PA6 around 220 °C: once the melting process starts, the modulus drops steeply and it is no longer possible to measure the tensile mechanical modulus with the DMTA apparatus due to the macroscopically fast flow of the sample. It is also interesting to note the presence of a second relaxation, before the final melting of the matrix ethylene-1-octene copolymer (Fig. 4(a)), associated to the motion of chain units within the crystalline portion, the so-called 'crystalline relaxation'. The α relaxation in polyethylenes is considered to be composed of two peaks, one of them attributed to an intralamellar slip process and the other one to intracrystalline chain motions [38–41].

Fig. 5 shows E' and tan δ for the different blends. For each of them, up to 100 °C the mechanical spectra are quite similar to those of the respective ethylene-1-octene copolymer matrices (Fig. 4(a)). However, once the matrix is melted, due to their dimensional stability, it is still possible to measure the tensile modulus of the samples B1 and B2 up to 200 °C, i.e. until the melting of the dispersed PA6 droplets starts. The measured E' values above the melting point of the matrix (higher than 1 MPa) are approximately comparable to those of crosslinked elastomers. However, this is not the expected behavior for a 'normal' blend with dispersed droplet morphology: one would expect no connection between the PA6 particles, and at temperatures above the melting range of the matrix the modulus is expected to drop due to flow of chains in the melt. The intriguing behavior of B1 and B2 at higher temperatures, i.e. the improved mechanical properties of

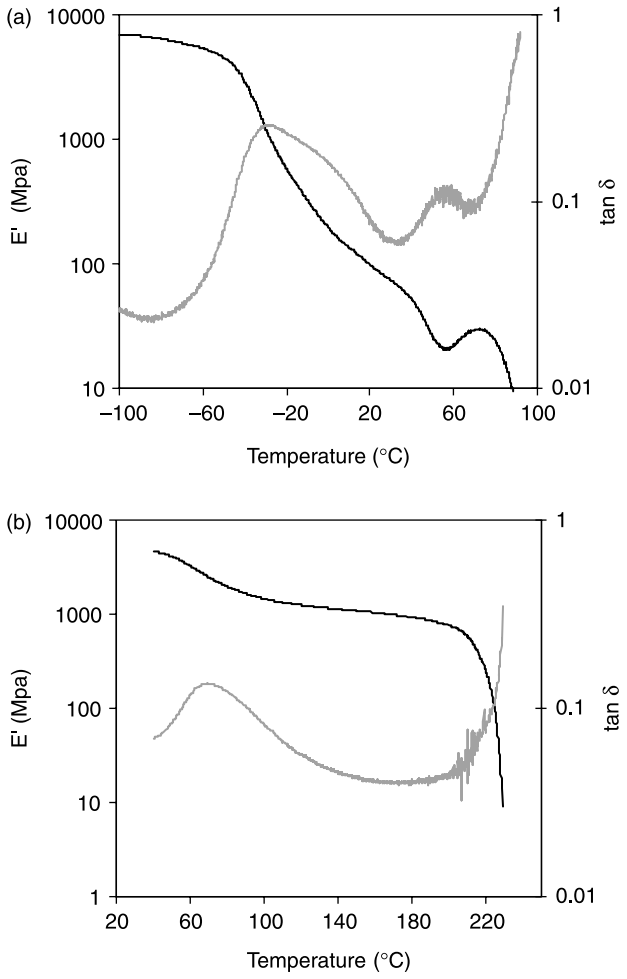

Fig. 4. Dynamic mechanical spectra for the bulk samples: (a) ethylene-1-octene copolymer (Exact® 8201) (b) PA6.

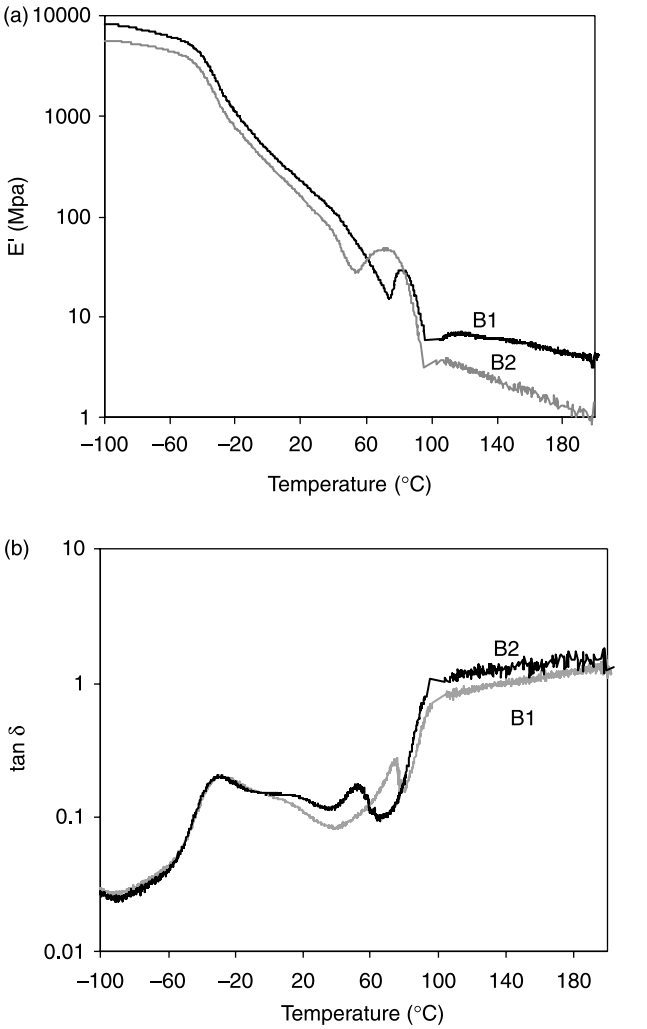

Fig. 5. Dynamic mechanical spectra for the different blends: (a) Storage modulus, E'. (b) Loss tangent, tan δ.

these samples compared to what would be expected in a conventional blend of the (qualitatively) same morphology and composition, allows extending their use to those applications in which dimensional stability is required at high temperatures. Moreover, due to the high supercoolings in these blends (as caused by the above described fractionated/homogeneous crystallization phenomenon), such system allows to be processed as polymer melts at temperatures as low as 140–160 °C coming from the melt: the same temperature range in which they will show such a relatively high mechanical modulus on heating.

The existence of a quasi-plateau in E' at high temperatures (Fig. 5(a)), especially for B1, could suggest the presence of a chemical network that somehow links the PA6 droplets accounting for the observed mechanical coherence above the melting point of the matrix. Nevertheless, this hypothesis fails after performing some simple experiments with solvents. It is found that toluene, a good solvent for the ethylene-1-octene copolymers (but not for PA6), is able to solve completely the polyethylene part of the blends. This solvent causes disintegration of the sample and only a milky, stable emulsion of very well compatibilized droplets remains after stirring at 50 °C for a few hours. The existence of some sort of chemical links between PA droplets would imply swelling rather than dissolution of the material. On the other hand, formic acid is a good solvent for PA6 (but not for the ethylene-1-octene copolymers); when the blends are immersed in this solvent the macroscopically consistence of the samples is kept but the external appearance of the sample changes due to extraction of surface droplets. If the diffusion of the solvent through the matrix could take place, to our opinion, it would be possible to extract the whole PA6 phase leaving the matrix intact. On the basis of these simple experiments, the existence of a chemical network that could account for the mechanical coherence of B1 and B2 at high temperatures has to be rejected. In other words: there is no co-continuous structure.

Besides, the presence of some kind of network would allow the application of the theory of rubber elasticity for its characterization. In the affine model, the average molar mass between crosslinks M_c (elastically active chains) is [42]

$$M_c = \frac{3\rho RT}{E'}, \tag{3}$$

where ρ is the density, R is the universal gas constant, T the absolute temperature and E' the modulus in the elastomeric region at T. The application of this equation above 100 °C to either B1 or B2 gives $M_c \sim 1.5$–2 kg/mol, a value too low to account for the distance between the dispersed PA6 droplets.

Seeking for an explanation of the peculiar mechanical behavior, let us consider in some detail the molecular architecture of the constituting chains, for example, B1. This blend consists of dispersed PA6 droplets of sizes ranging 200–500 nm (Figs. 1 and 2) and an average droplet distance of 100–200 nm. The compatibilizer being a key factor realizing a good dispersion of the PA6 droplets in the ethylene-1-octene copolymers matrix, its role in the mechanical properties of the blends is also important. The PE-*g*-MA used consists of polyethylene chains ($M_w = 65$ kg/mol) with 0.9-wt% of MA, i.e. around 4–6 MA groups per PE chain. It is known that PA6 is able to react with PE-*g*-MA to yield imides as linking group between PE and PA. Taking into account the PA6/compatibilizer ratio in our blends (the concentration of amine end groups in the PA6 is 43 ± 5 mequiv./kg), a simple calculation gives the anhydride/amine molar ratio to be around 0.5. It is known that in this situation only the end groups of the PA6 react (if the ratio was above 1.0, all the amines groups were converted first, but consequently the amide groups were hydrolysed resulting in PA6 chain scission and the formation of carboxylic acid and amine end groups) [43]. This mechanism suggests a physical picture of the system in which the PA6 droplets are surrounded by a shell of compatibilizer polyethylene chains that are chemically linked to the droplets at several points. Since, the nature of the compatibilizer and the matrix is quite similar, it is expected these shell chains to be highly entangled with the matrix chains, the more so the higher the molar mass of the matrix. Fig. 6 shows the chemical reaction between the compatibilizer and PA6 as well as a schematic representation of the described molecular situation.

The molecular architecture drawn suggests a system within a high density of physical entanglements. Since, occurrence of flow in the melt is related to the disentangling time [44], the matrix chains will flow but with a much slower dynamics than in case of a 'normal' polymer or blend: the flow dynamics of our system is decreased because the mobility of the compatibilizer chains is highly hindered due to their links to the PA6 droplets, which function as physical crosslinks in the system, while disentanglement of the matrix chains becomes more complicated and takes place on a much longer time scale.

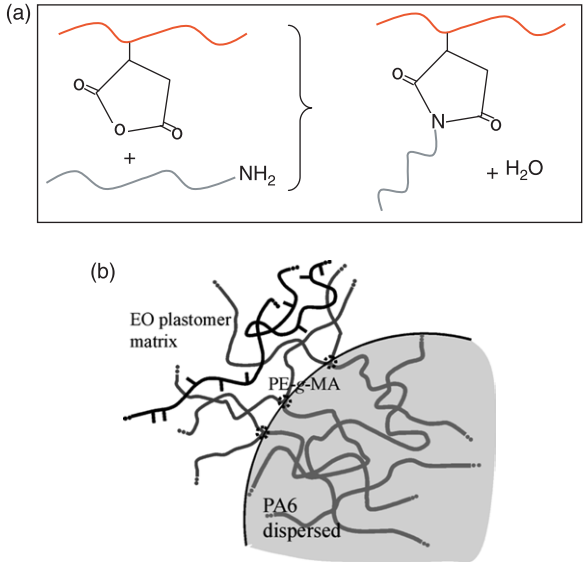

Fig. 6. (a) Chemical reaction between the compatibilizer and the amine group of the PA6 chains. (b) Sketch of the molecular situation. The shaded represents the PA6 dispersed phase, rounded shape in agreement with the microscope results. (◌) imide, ⊥ EO plastomer, — PA, —— PE-*g*-MA compatibilizer.

DMTA spectra support the molecular situation sketched. It is observed (Fig. 5) that once the matrix is melted, the modulus is not constant but decreases as temperature increases. At the same tame tan δ increases corresponding to an irreversible melt flow process. Besides, the mechanical behavior depends slightly on the average molar mass of the matrix: the lower the molar mass (the lower the viscosity, the higher MFI) the faster the dynamics of the flow process. E' decreases faster for B2 than for B1. The influence of the matrix on the morphology of the dispersed PA6 droplets (size and distance between droplets) is a double one: on the one hand a higher viscosity matrix (lower viscosity ratio) results in a better dispersion (unimodal distribution), on the other hand higher viscosity means higher molar mass (Table 1) resulting in a increase number of entanglements between matrix chains and compatibilizer chains: at least a fraction of PA6 droplets dispersed in B2 (bimodal distribution), within a matrix of much lower molar mass (Table 1), are bigger and far from each other; entanglements, being able to maintain the macroscopic coherence at higher temperatures, result in a lower modulus compared to B1.

A rheometer allows to compare the mechanical properties of the blends and the base components at higher temperatures than what it is possible with the DMTA device, which is in need of dimensional stability for measuring. Fig. 7 shows G' and tan δ as a function of temperature for each one of the blends and the ethylene-1-octene copolymer. Once the matrix has melted G' decreases as temperature increases. At any temperature, G' is higher for B1 than for B2. This fact stresses the importance of the physical properties of the matrix for the mechanical behavior: the same amount of PA6 is dispersed in both B1 and B2; nevertheless, E' differs between them almost one order of magnitude at high temperatures. Furthermore, G' values for B1 and B2 show the importance of the average molar mass of the matrix: even though the droplet size distribution is quite similar in both cases (Figs. 1 and 2), due to the lower molar mass of the ethylene-1-octene copolymer matrix in B2, the entanglement density is lower and so the mechanical modulus is lower at higher temperatures. On the other hand, the evolution of the loss tangent accounts for the irreversible 'degree of flow' in the material: tan δ is null for a true network and it increases as the crosslink density decreases, i.e. as chain flow progresses.

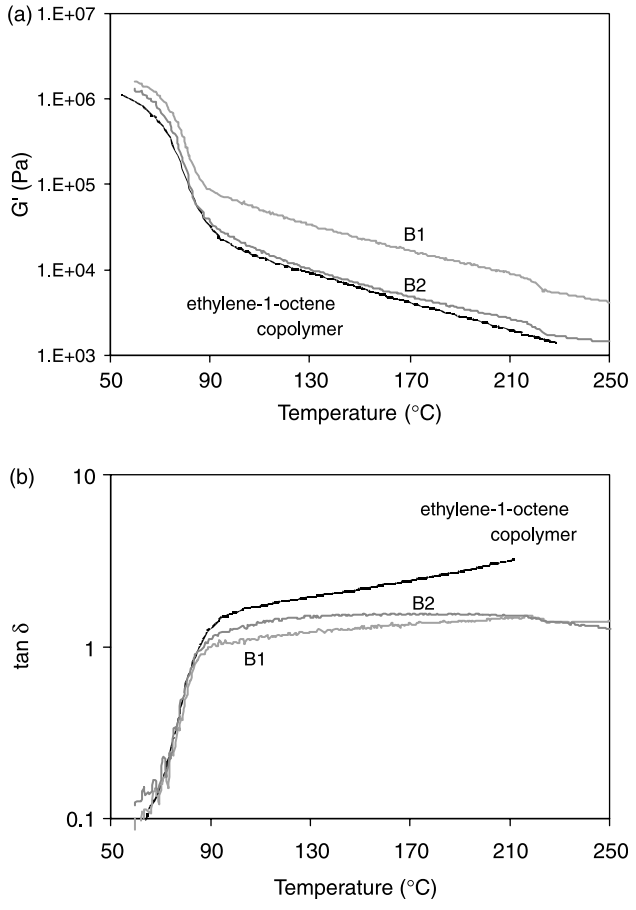

Fig. 7. Rheological measurements for the different blends and the base ethylene-1-octene copolymers (Exact® 8201). (a) Shear storage modulus G' and (b) loss tangent, tan δ.

The frequency sweeps at different temperatures also supports the idea of a system with a slowed down flow dynamics. Fig. 8 shows G' and G'' shifted to a reference temperature of $T_{ref}=150\,^{\circ}C$ using the time–temperature superposition principle [45] both for the base ethylene-1-octene copolymer and the blend B1. The inset in Fig. 8 shows the horizontal shift factor, a_T, following the Arrhenius dependence for the ethylene-1-octene copolymer melt and some deviation from linearity, specially at high temperatures, for the blend B1. This non-linear dependence for a_T can be justified by the presence of the (non-melted) PA6 droplets that modify the viscoelastic properties of the system even if the matrix is in the melt state. The use of the time–temperature-superposition principle can be justified so as to achieve a better comparison between systems for the frequency dependence at longer times. Vertical shifts factors are close to unity in any case. It can be checked that, for a fixed temperature, the modulus is not constant (as it would be in case of a chemical network) but decreases as frequency does. The effect of temperature is to shift the curves to lower G' values without modifying its shape appreciably. This is no longer the case in 'normal' systems. It is clearly observed that while the same frequency dependence at longer times is kept for B1 as temperature increases ($G'\sim\omega^{0.5}$ Fig. 8(b)) the slope of G' for the ethylene-1-octene copolymer base material increases as temperature does reaching the characteristic $G'\sim\omega^2$ dependence of a melt in the limit of low frequency (at high temperatures) [46–48].

The rheological behavior of the blends is similar to that of a material near a gelation point. The gel point can be extracted by presenting the data in terms of the loss tangent and looking for the frequency independence of slow power law dynamics [49,50]. Fig. 9(a) shows tan δ versus ω for the ethylene-1-octene copolymer at different temperatures. The loss tangent increases as temperature does, reaching the characteristic limiting slope of -1 at low frequencies, at the higher temperature. This is the typical linear viscoelastic behaviour of the melt. The frequency dependence of the loss angle is different for the blend. The low frequency flat region in the loss angle is said to be associated with the gel point [49,50]. The

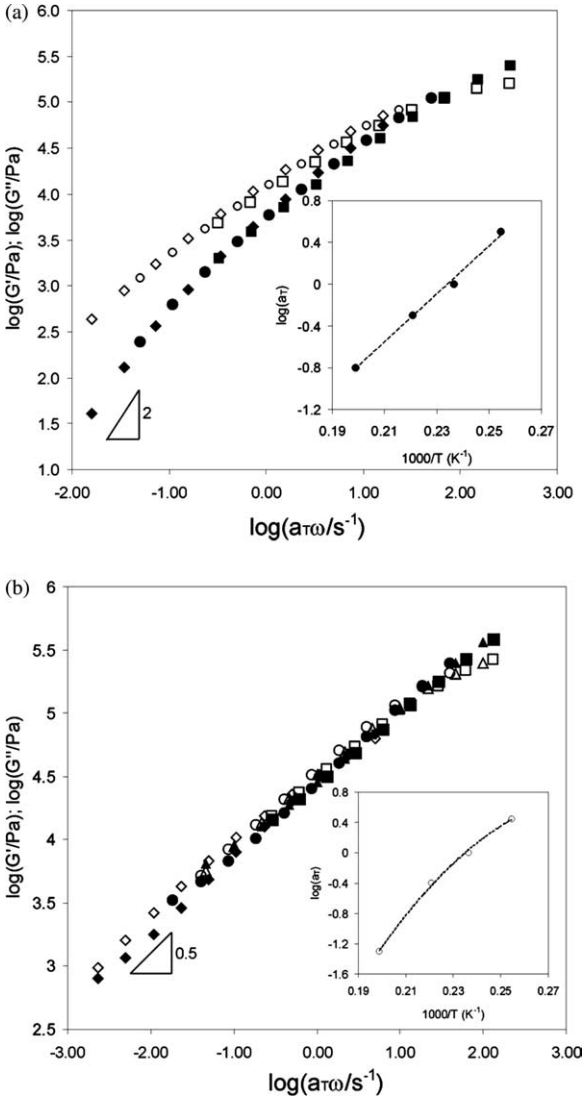

Fig. 8. Storage modulus, G' (filled symbols), and loss modulus, G'' (open symbols), master curves of the (a) base ethylene-1-octene copolymer (Exact® 8201) and (b) blend B1 at $T_{ref}=150$ °C. The frequency sweeps data were taken at temperatures 120 (■), 150 (▲), 180 (♦) and 230 (●) °C. The insets show the horizontal temperature shift factor at $T_{ref}=150$ °C versus inverse temperature.

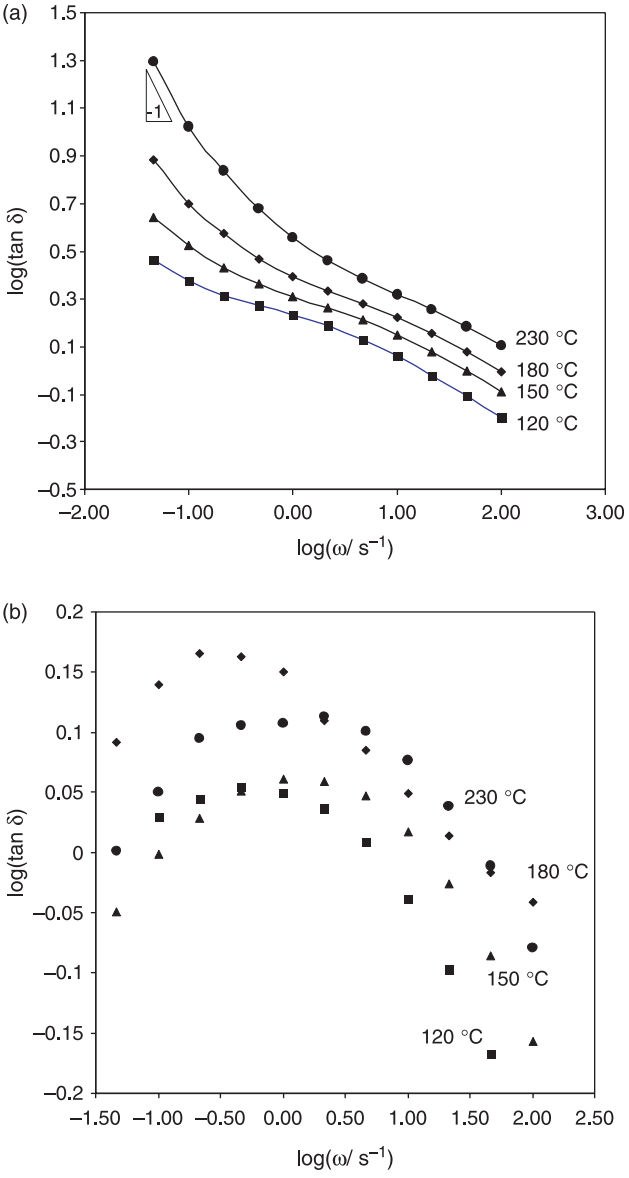

Fig. 9. Loss tangent versus frequency at different temperatures for B1 (b) and its ethylene–1–octene copolymer matrix (a) 120 (■), 150 (▲), 180 (♦) and 230 (●) °C. The limiting slope of −1 at low frequencies is shown for comparison in (a).

decrease of the loss tangent curve at low frequencies is considered to be a characteristic feature of a material above the gel point. The viscoelastic properties of the dispersed systems are likely to be those of a physical gel, even if the matrix is in the melt state and there is no physical connection between the dispersed droplets.

4. Conclusions

The present work introduces for the first time a polymer blend (ethylene-1-octene copolymer/PE-*g*-MA/PA6 ratio 62.5/7.5/30) with a droplet dispersed morphology that shows good mechanical properties above the melting point of the ethylene-1-octene copolymers matrix. The mechanical response depends on the molar mass of the matrix employed: as the molar mass decreases, the mechanical modulus decreases but is still able to maintain dimensional stability.

Because chemical connection between the PA6 droplets has been discarded on the basis of swelling experiments, the explanation of the intriguing behavior of the blends has to be found in the molecular architecture of the constituting chains. It is known that the compatibilizer chains are on the one hand chemically linked to the PA6 droplets at several points (several MA groups per chain) and on the other hand are highly entangled with the matrix chains, the more so the higher the molar mass of the matrix (the lower the MFI). Since, occurrence of flow in the melt is related to the disentanglement time, the flow dynamics of our system is decreased because the mobility of the compatibilizer chains is highly hindered due to their links to the PA6 droplets, that function as physical

crosslinks in the system. Summarizing, the accumulation of three factors accounts for the mechanical behavior of these blends: (1) the very fine dispersion of the droplets in the matrix, (2) the hindered mobility of the compatibilizer chains connected to the droplets and (3) the increased number of entanglements in case of high average molar mass of the matrix chains. Both DMTA spectra and rheology frequency sweeps measurements support this physical picture.

Besides, due to the fine dispersion of the PA6, fractionated/homogeneous crystallization takes place, resulting in an extra supercooling of around 50 °C compared to the PA6 bulk crystallization temperature. From an application point of view this crystallization behavior allows the system to be processed as a polymer melt at temperatures as low as 140–160 °C coming from the melt. Nevertheless, melting of the droplets takes place at temperatures close to that of the bulk polyamide around 220 °C and, on heating, the systems shows improved mechanical stability at the same temperature range.

Acknowledgements

M.S.S. wishes to acknowledge the Programa de Incentivo a la Investigación and the Universidad Politécnica de Valencia for financial support for his stay at the Katholieke Universiteit Leuven.

References

[1] Bruls W, Repin J, Widdershoven C. Patent WO03087216, 2003.
[2] Kudva RA, Keskkula H, Paul DR. Polymer 1999;40:6003.
[3] Pesetskii SS, Krivoguz YM, Jurkowski B. J Appl Polym Sci 2004;92:1702.
[4] Scaffaro R, La Mantia FP, Canfora L, Polacco G, Filippi S, Magagnini P. Polymer 2003;44:6951.
[5] Chiono V, Filippi S, Yordanov Hr, Minkova L, Magagnini P. Polymer 2003;44:2423.
[6] Yordanov Hr, Minkova L. Eur Polym J 2003;39:951.
[7] Li QF, Him DG, Wu DZ, Lu K, Jin RG. Polym Eng Sci 2001;41:2155.
[8] Tasdemir M, Yildirim H. J Appl Polym Sci 2001;82:1748.
[9] Yao ZH, Yin ZH, Sun G, Liu CZ, Tong J, Ren LQ, et al. J Appl Polym Sci 2000;75:232.
[10] Burgisi G, Paternoster M, Peduto N, Saraceno A. J Appl Polym Sci 1997;66:777.
[11] Raval H, Devi S, Singh YP, Mehta MH. Polymer 1991;32:493.
[12] Premphet-Sirisinha K, Chalearmthitipa S. Polym Eng Sci 2003;43:317.
[13] Minkova L, Yordanov Hr, Filippi S. Polymer 2002;43:6204.
[14] Bai SL, Wang GT, Hiver JM, G'Sell C. Polymer 2004;45:3063.
[15] Okada O, Keskkula H, Paul DR. Polymer 1999;40:2699.
[16] Okada O, Keskkula H, Paul DR. Polymer 2001;42:8715.
[17] Tedesco A, Barbosa RV, Nachtingall SMB, Mauler RS. Polym Test 2002;21:11.
[18] Padwa AR. Polym Eng Sci 1992;32:1703.
[19] Lim S, White JL. Polym Eng Sci 1994;34:221.
[20] Serpe G, Jarrin J, Dawans F. Polym Eng Sci 1990;30:553.
[21] Hobbs SY, Bopp RC, Watkins VH. Polym Eng Sci 1983;23:380.
[22] Kim BK, Park SY, Park SJ. Eur Polym J 1991;27:349.
[23] Gonzalez MA, Keskkula H, Paul DR. Polymer 1995;36:4587.
[24] Rosch J. Polym Eng Sci 1995;35:1917.
[25] Abbate M, Diliello V, Martuscelli E, Musto P, Ragosta G, Scarinzi G. Polymer 1992;33:2940.
[26] Wilkinson A, Clemens ML, Harding VM. Polymer 2004;45:5239.
[27] Karssenberg FG, Mathot VBF, Zwartkruis TJG. J Polym Sci, Polym Phys Ed 2006;44:722.
[28] Everaert V, Groeninckx G, Aerts L. Polymer 2000;41:1409.
[29] Vanden Eynde S, Mathot VBF, Koch MHJ, Reynaers H. Polymer 2000;4:4889.
[30] Goderis B, Peeters M, Mathot VBF, Koch MHJ, Bras W, Ryan AJ, et al. J Polym Sci, Polym Phys Ed 2000;38:1975.
[31] Mathot VBF, Reynaers H. Crystallization, melting and morphology of homogeneous ethylene copolymers. In: Cheng SZD, editor. Handbook of thermal analysis and calorimetry. Applications to polymers and plastics, vol. 3. Amsterdam: Elsevier; 2002. p. 197.
[32] Hu W, Mathot VBF. Macromolecules 2004;37(2):673.
[33] Frensch H, Harnischfeger P, Jungnickel BJ. In: Utracki LA, Weiss RA, editors. Multiphase polymers: blends and ionomers. ACS symposium series, vol. 395; 1989, 1989. p. 101.
[34] Groeninckx G, Vanneste M, Everaert V. In: Utracki LA, editor. Polymer blends handbook. Crystallization, morphological structure and melting of polymer blends, vol. 1. Dordrecht: Kluwer Academix Publishers; 2002. p. 203–94 [chapter 3].
[35] Tol RT, Mathot VBF, Reynaers H, Groeninckx G. Phase morphology and interfaces in micro and nanostructured immiscible polymer blend systems. In: Harrats C, Thomas S, Groeninckx G, editors. Interrelation between phase morphology, crystallization and semicrystalline structure in immiscible polymer blends. Confined crystallization phenomena in micro- and nanometer sized droplets. USA: CRC Press; 2005. p. 391–420 [chapter 12].
[36] Arnal ML, Müller AJ. Macromol Chem Phys 1999;200:2559.
[37] Tol RT, Mathot VBF, Groeninckx G. Polymer 2004;46:369.
[38] Kyu T, Yasuda N, Suehiro S, Nomura S, Kawai H. Polym J 1976;8:565.
[39] Suehiro S, Yamada T, Inagaki H, Kyu T, Nomura S, Kawai H. J Polym Sci, Polym Phys Ed 1979;17:763.
[40] Tanaka A, Chang EP, Delf B, Kimura T, Stein RS. J Polym Sci, Polym Phys Ed 1973;11:1891.
[41] Nitta K-H, Tanaka A. Polymer 2001;42:1219.
[42] Flory PJ. Principles of polymer chemistry. Ithaca, NY: Cornell University Press; 1953.
[43] Van Duin M, Borggreve RJM. In: Al-Malaika S, editor. Reactive modifiers for polymers. London: Blackie Academic and Professional; 1997.
[44] Strobl G. The physics of polymers. Berlin: Springer; 1997 [chapter 5].
[45] Ferry JD. Viscoelastic properties of polymers. New York: Wiley; 1980.
[46] Macosko CW. Rheology. Principles, measurements and applications. New York: VCH Publishers; 1994 [chapter 3].
[47] Muthukumar M, Winter HH. Macromolecules 1986;1955.
[48] Vilgis TA, Winter HH. Colloid Polym Sci 1988;266:494.
[49] Schwittay C, Mours M, Winter HH. Faraday Discuss 1995;101:93.
[50] Pogodina NV, Winter H. Macromolecules 1998;31:8164.